RhoA, Rac1, and Cdc42 differentially regulate αSMA and collagen I expression in mesenchymal stem cells

Received for publication, November 27, 2017, and in revised form, April 9, 2018 Published, Papers in Press, April 26, 2018, DOI 10.1074/jbc.RA117.001113

Jianfeng Ge[‡], Laurent Burnier[‡], Maria Adamopoulou[‡], Mei Qi Kwa[‡], Matthias Schaks[§¶], Klemens Rottner[§¶], and Cord Brakebusch[‡1]

From the [‡]Biotech Research and Innovation Center (BRIC), University of Copenhagen, Ole Maaløes vej 5, 2200 Copenhagen, Denmark, the [§]Zoological Institute, Technische Universität Braunschweig, Spielmannstrasse 8, 38106 Braunschweig, Germany, and the [¶]Department of Cell Biology, Helmholtz Centre for Infection Research, Inhoffenstrasse 7, 38124 Braunschweig, Germany

Edited by Amanda J. Fosang

Mesenchymal stem cells (MSC) are suggested to be important progenitors of myofibroblasts in fibrosis. To understand the role of Rho GTPase signaling in TGFβ-induced myofibroblast differentiation of MSC, we generated a novel MSC line and its descendants lacking functional Rho GTPases and Rho GTPase signaling components. Unexpectedly, our data revealed that Rho GTPase signaling is required for TGFβ-induced expression of α-smooth muscle actin (αSMA) but not of collagen I α1 (*col1a1*). Whereas loss of RhoA and Cdc42 reduced αSMA expression, ablation of the Rac1 gene had the opposite effect. Although actin polymerization and MRTFa were crucial for TGFβ-induced αSMA expression, neither Arp2/3-dependent actin polymerization nor cofilin-dependent severing and depolymerization of F-actin were required. Instead, F-actin levels were dependent on cell contraction, and TGFβ-induced actin polymerization correlated with increased cell contraction mediated by RhoA and Cdc42. Finally, we observed impaired collagen I secretion in MSC lacking RhoA or Cdc42. These data give novel molecular insights into the role of Rho GTPases in TGFβ signaling and have implications for our understanding of MSC function in fibrosis.

Fibrosis, the excessive production of collagen I and other extracellular matrix (ECM)[2] proteins, is an important clinical problem with few treatment options (1, 2). In the liver, fibrosis caused by viral hepatitis, alcohol, or obesity can lead to liver failure and increase the likelihood for liver cancer (3). However, fibrosis occurs also in many other tissues such as kidney, heart, and lungs and leads to organ failure due to functional impairment. The major cell type responsible for pathological ECM production is the myofibroblast, which can be described as a contractile, collagen I-producing, fibroblastoid cell, characterized mostly by high expression of α-smooth muscle actin (αSMA; gene name, *ACTA2*) (4). The biology of myofibroblasts is complex, because apparently many different precursor populations are able to differentiate into myofibroblasts, including tissue-resident fibroblasts and epithelial cells, which may result in different subtypes of myofibroblasts with different biological properties. The extent to which each progenitor population contributes to myofibroblasts in disease is debated and might be dependent on the tissue as well as on the stimulus. Recently, vascular mesenchymal stem cell-like cells (MSC) were described as critically important myofibroblast precursors in different murine fibrosis models (5). This originally small population, present in all vascularized tissues, expands strongly during disease and gives rise to a large share of the differentiated myofibroblasts. Moreover, the elimination of this population strongly reduces the development of kidney and heart fibrosis. It is important therefore to understand the mechanisms that trigger the differentiation of MSC into myofibroblasts. *In vitro*, TGFβ can induce myofibroblast differentiation of MSC derived from adipose or prostate tissue, as characterized by αSMA and collagen I expression (6, 7). TGFβ signaling is complex and can be divided into a canonical part that is dependent on the Smad2/3/4 transcription factors and a less characterized non-canonical part, which includes activation of the small Rho GTPase RhoA (8). The latter has been shown to regulate actin polymerization via ROCK (9), triggering nuclear translocation of the transcription co-factor MRTFa, which then binds to the transcription factor SRF triggering the expression of αSMA and collagen I in fibroblasts (10–12). How TGFβ signaling activates RhoA, how ROCK is controlling F-actin formation, and how SRF-MRTF synergizes with Smad2/3/4 canonical signaling is not well-understood. It is also not clear to what extent other major regulators of actin polymerization such as the small GTPases Rac1 and Cdc42 might play a role in MRTFa activation during myofibroblast differentiation.

To increase the understanding of the molecular pathways underlying fibrotic disease, we set out to investigate how TGFβ-induced myofibroblast differentiation is regulated in the pathophysiologically relevant precursor population of MSC. Importantly, we tested how the Rho GTPases RhoA, Rac1, and Cdc42 affect MSC differentiation into the myofibroblast and which signal transduction pathways are involved downstream

This work was supported in part by the Novo Nordisk Foundation (to L. B.) and Grant GRK2223/1 from the Deutsche Forschungsgemeinschaft (to K. R.). The authors declare that they have no conflicts of interest with the contents of this article.

This article contains Figs. S1–S10, Table S1, and Movies 1–4.

[1] To whom correspondence should be addressed. Tel.: 45-353-25619; Fax: 45-353-25699; E-mail: cord.brakebusch@bric.ku.dk.

[2] The abbreviations used are: ECM, extracellular matrix; αSMA, α-smooth muscle actin; MSC, mesenchymal stem cell; TGFβ, transcription growth factor β; SRF, serum response factor; MRTF, myocardin-related transcription factor; ERK, extracellular signal-regulated kinase; JNK, c-Jun N-terminal kinase; gRNA, guide RNA; TBS, Tris-buffered saline; qRT-PCR, quantitative RT-PCR; LIMK, LIM domain kinase; ROCK, Rho-associated coiled-coil–containing protein kinase.

© 2018 by The American Society for Biochemistry and Molecular Biology, Inc. Published in the U.S.A.

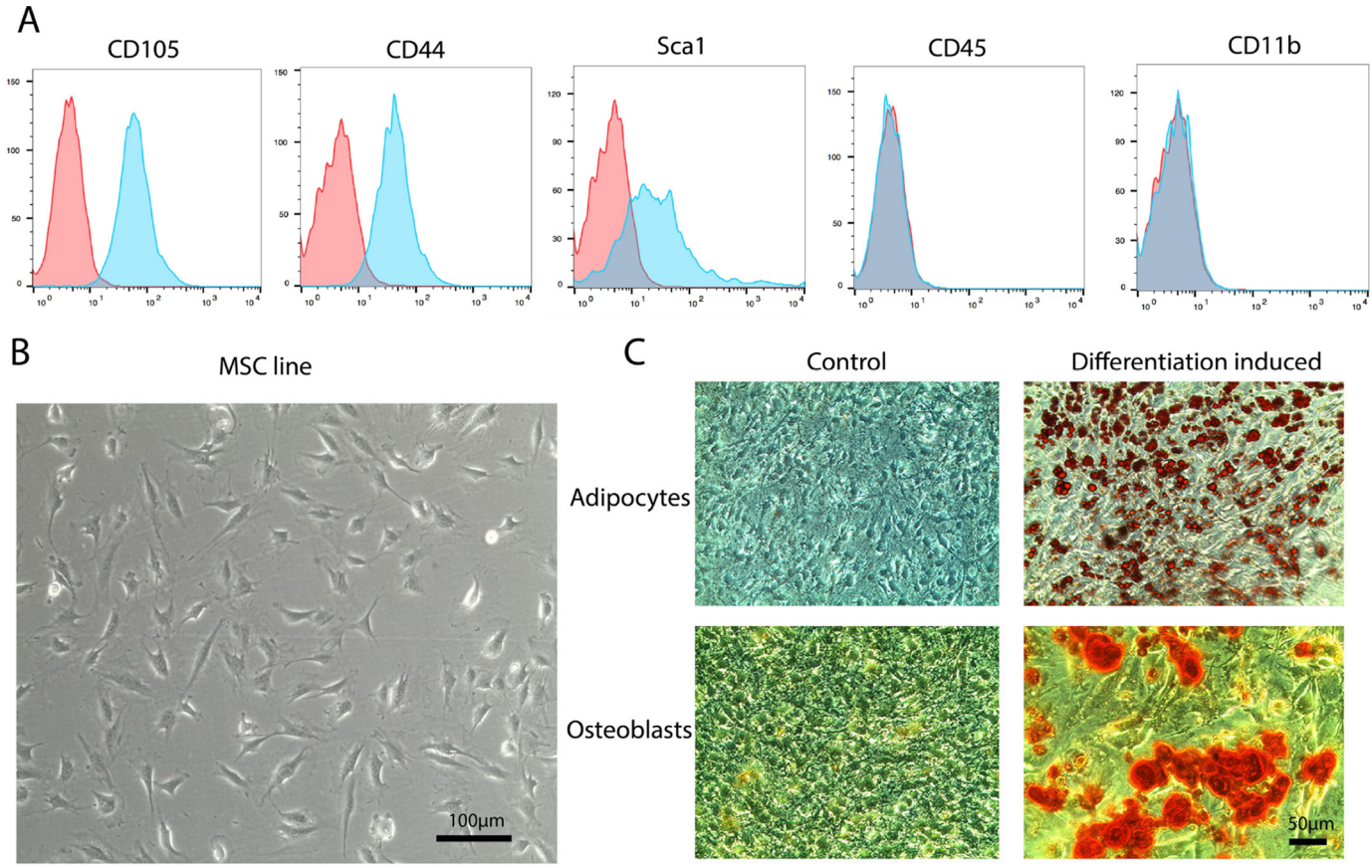

Figure 1. Establishment of a spontaneously immortalized MSC line. *A*, FACS analysis of p58 MSC for surface markers of MSC (CD105, CD44, and Sca1) and hematopoietic cells (CD45 and CD11b). Autofluorescence is shown in *red* ($n = 3$). *B*, bright field microscopy of MSC. *C*, differentiation of p58 MSC to adipocytes and osteoblasts stained with Oil Red O (adipocytes, fat vesicles shown in *red*) and Alizarin Red S (osteoblasts, *orange-red*) ($n = 4$).

of Rho GTPases. Our results indicate important roles for RhoA, Rac1, and Cdc42 in controlling TGFβ-induced expression of the myofibroblast differentiation marker αSMA in MSC but showed surprisingly little effect on the regulation of *col1a1* mRNA. TGFβ-induced regulation of αSMA expression depended on contraction, but independently of cofilin, in contrast to previous suggestions. These data give important insights into myofibroblast differentiation of a disease-relevant progenitor population, which may help to find novel treatments preventing fibrosis in different tissues.

Results

Establishment of a spontaneously immortalized MSC line

Standard preparations of primary mouse MSC are contaminated with other cell types at low passage numbers and prone to senescence upon longer passaging, leaving only a small window for experimentation. We therefore established a spontaneously immortalized murine MSC line from bone-derived MSC. After 58 passages, the MSC line showed high expression of the murine MSC surface markers CD105, CD44, and Sca1, whereas no contaminating hematopoietic cells expressing CD45 or macrophages expressing CD11b could be detected by FACS (Fig. 1*A*). Light microscopy revealed a fibroblast-like triangular cell morphology similar to primary MSC (Fig. 1*B*). Moreover, the MSC showed efficient differentiation into adipocytes and osteoblasts in the respective differentiation media (Fig. 1*C*). Moreover, no differentiation into these cell types was detectable under normal growth conditions.

These data indicate that the established MSC line displays major hallmarks of primary MSC at least up to passage 58. Further experiments were carried out with cells from passage 42 to 47.

Canonical TGFβ signaling triggers myofibroblast differentiation of MSC

TGFβ promotes the differentiation of fibroblasts into myofibroblasts, characterized by expression of αSMA and collagen I. MSC are assumed to behave similarly but have to date been tested only for αSMA expression in response to TGFβ1. Treatment of our MSC line with TGFβ1 indeed resulted in effective up-regulation of both αSMA and *col1a1* mRNA after 24 h (Fig. 2, *A* and *B*). To investigate the dependence of this differentiation on canonical Smad-related TGFβ signaling, we established MSC lines lacking Smad2, Smad3, or Smad4 using lentiviral CRISPR/Cas-mediated genome editing and confirmed the absence of respective proteins by Western blotting (Fig. 2*C*). Deletion of Smad2 or Smad3 alone showed little effect, but ablation of the Smad4 gene effectively abrogated TGFβ-induced expression of αSMA or *col1a1* (Fig. 2, *D–F*). Basal expression of αSMA and *col1a1* was not significantly altered by the loss of Smad4.

These results demonstrate an essential role for canonical Smad4-dependent TGFβ signaling for myofibroblast differentiation of MSC, whereas Smad2 or Smad3 are not required and

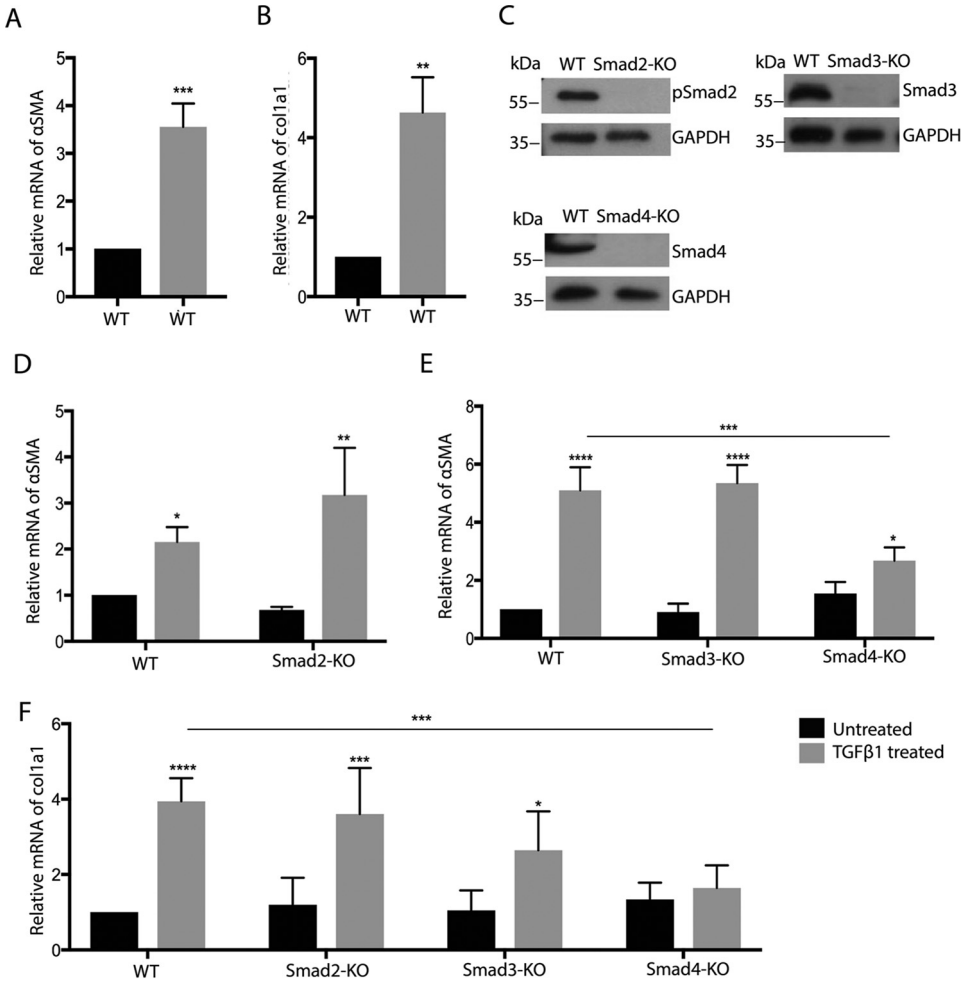

Figure 2. Canonical TGFβ signaling is required for myofibroblast differentiation of MSC. *A*, *B*, and *D–F*, qRT-PCR analysis for the indicated genes of WT, Smad2-KO, Smad3-KO, and Smad4-KO cells (*black bars*, 24-h TGFβ; *gray bars*, untreated; $n = 3/3$). *C*, representative Western blotting for the indicated proteins of MSC with knockout of Smad2, Smad3, and Smad4. ****, $p < 0.0001$.

probably have redundant functions, in line with earlier observations in other cell types.

Rho GTPases control myofibroblast differentiation of MSC

Treatment of MSC with TGFβ resulted in increased phosphorylation of Smad2 and the Rho GTPase downstream effectors MLC2 (in particular RhoA but also Rac1 and Cdc42), Pak1 (Rac1 and Cdc42), and Pak4 (Cdc42), suggesting that TGFβ induces Rho GTPase activation in parallel with canonical TGFβ signaling (Fig. S7). Kinetic analysis indicated a high and significant activation of Smad2, PAK1, and Pak4 after 24 h and of MLC2 after 2 h. To analyze the functional role of basal and TGFβ-induced Rho GTPase signaling in the TGFβ-induced myofibroblast differentiation of MSC, we established MSC lines lacking RhoA, Rac1, or Cdc42 by CRISPR/Cas9-mediated genome editing.

Although RhoA and Cdc42 were efficiently deleted, the loss of Rac1 protein was not complete, indicating the presence of a minor amount of nonrecombined cells (Fig. 3*A*). This was most likely because of the severely reduced growth of Rac1-null MSC, giving nonrecombined cells a competitive advantage in the polyclonal cell mixture (data not shown). MSC suppressed for RhoA, Rac1, or Cdc42 expression showed morphologies similar to fibroblastoid cells lacking these Rho GTPase genes (Fig. 3*B*). Time-lapse migration assays revealed that Rac1-null MSC are hardly motile, whereas the long, thin extensions of Cdc42-null cells seen in still images (Fig. 3*B*) were observed to rupture during migration, leaving behind small patches of cytoplasm on cell tracks (Movies 1–4). RhoA-null MSC were also more elongated than WT cells, and at least a subpopulation of cells displayed extended rear edges. With respect to their differentiation potential, we found that the loss of Rho GTPases did not prevent or induce the differentiation of MSC to adipocytes or osteoblasts (Fig. S6). Furthermore, none of the Rho GTPase KO MSC lines showed altered phosphorylation of Smad2 after 24-h treatment with TGFβ (Fig. 3, *C* and *D*), suggesting normal activation of TGFβR kinase activity, crucial for both canonical and noncanonical signaling.

TGFβ-induced expression of αSMA was significantly decreased in RhoA KO and Cdc42 KO MSC after 24-h stimulation, whereas the loss of Rac1 increased basal αSMA expression strongly (Fig. 4*A*). With respect to -fold change, only Cdc42 KO resulted in a significantly reduced induction (Table S1). After 3-day TGFβ treatment, the protein levels of αSMA were significantly lower in RhoA KO and Cdc42 KO cells compared with WT MSC, whereas no clear difference was detectable in Rac1 KO MSC (Fig. 4, *B* and *C*). To check whether constitutively

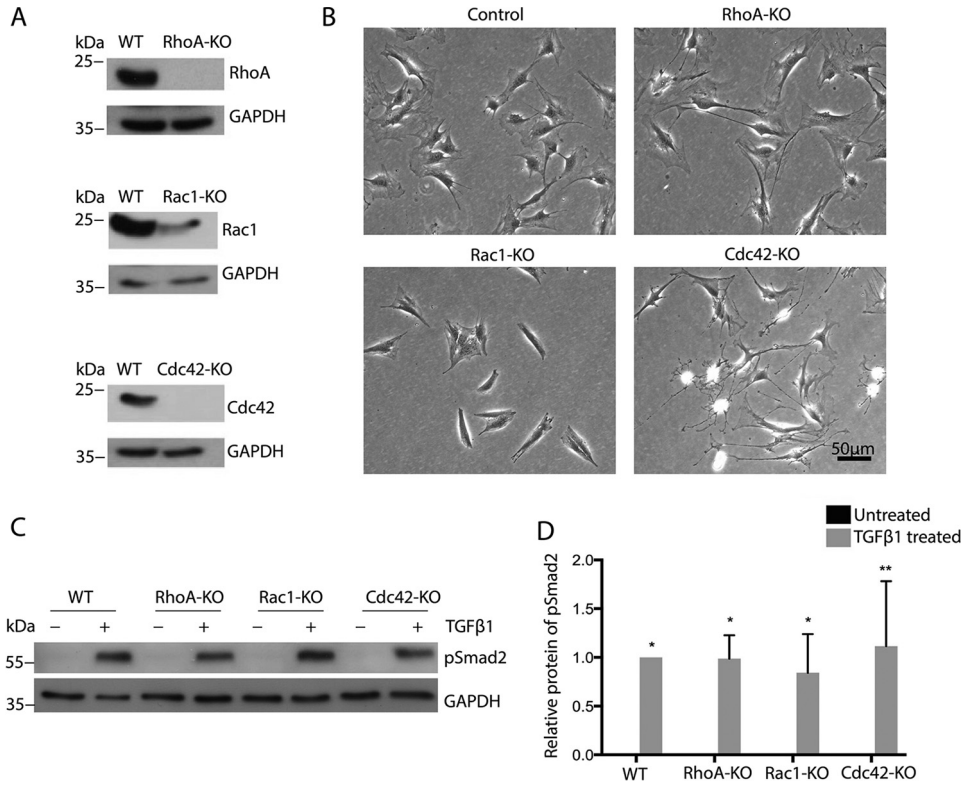

Figure 3. Rho GTPase-deficient MSC show clear morphological changes but normal Smad2 phosphorylation in response to TGFβ. *A*, representative Western blotting for the indicated proteins of MSC with knockout of RhoA, Rac1, and Cdc42. *B*, bright field microscopy of MSC with indicated gene deletions. *C* and *D*, representative Western blotting and quantification of lysates of indicated cells for pSmad2 (*black bars*, 24-h TGFβ; *gray bars*, untreated; $n = 3/3$).

active Rho GTPase mutants show effects opposite to the KO, we overexpressed fast-cycling mutants of RhoA, Rac1, and Cdc42 (35) in MSC and tested the effect on TGFβ-induced αSMA expression. Fast-cycling mutants (fcRho GTPases) are able to cycle between a GDP-bound and a GTP-bound form but are mostly in the GTP-bound form. Lentiviral transduction of MSC resulted in a high percentage of fast-cycling mutant expressing cells, as determined by co-expressed EGFP (Fig. S9, *A* and *B*). fcRhoA increased TGFβ-induced αSMA (Fig. S9, *E* and *F*), thus showing opposite effects than KO of RhoA, while fcRac1 prevented TGFβ-induced αSMA expression. fcCdc42 MSC behaved similar to control cells, suggesting that although a basal Cdc42 activity is required for myofibroblast activation, superactivation of Cdc42 is not having an extra effect.

Surprisingly, the deletion of RhoA in MSC showed no influence on TGFβ-induced *col1a1* mRNA expression (Fig. 4*D*), although RhoA is reportedly required for collagen 1 expression in fibroblasts (12). The loss of Rac1 or Cdc42 resulted in slightly reduced *col1a1* levels after 1-day stimulation (Fig. 4*D*). However, after 3-day stimulation, the deletion of Cdc42 did not cause any change in *col1a1* mRNA expression (Fig. 4*E*).

Following analysis of the cellular and secreted collagen 1 protein, both RhoA KO and Cdc42 KO MSC displayed an intracellular accumulation of cellular collagen 1 (Fig. 4, *F* and *G*). Moreover, secreted collagen 1 was significantly reduced in the supernatant of Cdc42-null MSC (Fig. 4, *F* and *H*).

These data indicate that both RhoA and Cdc42 are required for TGFβ-induced αSMA expression, whereas Rac1 plays an inhibitory role. They furthermore suggest a role for RhoA and Cdc42 in collagen I secretion but no or only a minor role in the regulation of *col1a1* mRNA.

Defective αSMA induction in Rho GTPase KO correlates with changes in F-actin and pMLC2

To identify changes in downstream components of Rho GTPase signaling that might correlate with the defective induction of αSMA, we first analyzed F-actin levels by quantifying cell staining with fluorescently labeled phalloidin. TGFβ treatment of control MSC induced a clear increase in F-actin in control but not in in RhoA KO and Cdc42 KO MSC (Fig. 5*A* and Fig. S1). Rac1 KO MSC, on the other hand, showed increased levels of F-actin in both the presence and absence of TGFβ (Fig. S1). These changes in F-actin correlated with changes in pMLC2, which is a marker for cell contraction (Fig. 5*B*). MSC expressing fcRhoA showed increased TGFβ-induced pMLC2, while fcRac1 and fcCdc42 MSC showed no significant changes (Fig. S9, *C* and *D*).

ADF/cofilin family members are important regulators of F-actin by severing it and promoting depolymerization with cofilin-1 (cofilin) as the major form in nonmuscle tissues. Cofilin is known to be inactivated by phosphorylation downstream of RhoA, Rac1, and Cdc42. However, we could not detect any significant changes in cofilin phosphorylation in MSC lacking these Rho GTPases after 24 h of treatment with TGFβ (Fig. 5*C* and Fig. S2). p38, ERK, and JNK are described as phosphorylated and activated by noncanonical TGFβ signaling (36). Testing pERK and pp38 after 24 h of TGFβ treatment, no significant TGFβ-dependent stimulation and no Rho GTPase-dependent

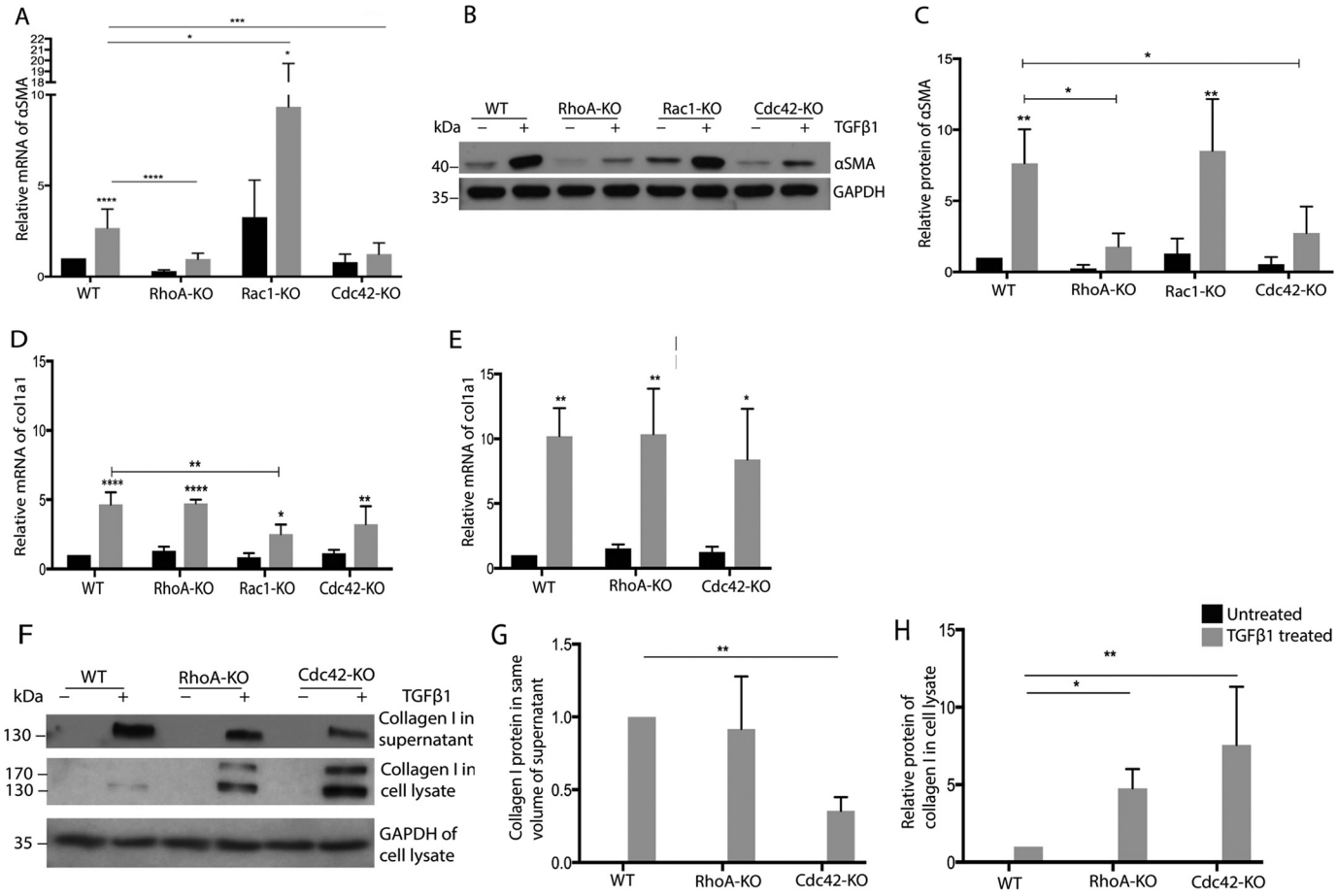

Figure 4. Rho GTPases regulate TGFβ-induced expression of αSMA but not of *col1a1*. *A*, *D*, and *E*, qRT-PCR analysis for indicated genes of RhoA-KO, Rac1-KO, Cdc42-KO, and WT cells after treatment for 24 h (*A* and *D*) or 3 days (*E*) with TGFβ (*black bars*, 24-h TGFβ; *gray bars*, untreated; $n = 6/6$). *B*, *C*, and *F–H*, representative Western blotting and quantification of lysates of indicated cells for αSMA (*B* and *C*) and collagen I (*F–H*) (*black bars*, 24-h TGFβ; *gray bars*, untreated; $n = 4/4$). ****, $p < 0.0001$.

alteration were detectable (Fig. 5, *D* and *E*, and Fig. S2). Unexpectedly, the p54 isoform of pJNK was increased in untreated and TGFβ-treated Cdc42 KO MSC, whereas RhoA KO cells showed no change (Fig. 5, *F* and *G*, and Fig. S2).

TGFβ-induced actin polymerization controls αSMA but not col1a1 expression

In fibroblasts, actin polymerization promotes nuclear translocation of the transcription factor MRTFa, which induces expression of both αSMA and collagen 1 (10, 11). In MSC, TGFβ treatment increased the formation of F-actin stress fibers over 24 h, visualized by fluorescent LifeAct (Fig. S8). We therefore investigated whether this pathway plays a related role in MSC. Inhibition of actin polymerization in MSC by latrunculin abrogated basal αSMA as well as induced αSMA expression and caused a partial reduction of TGFβ-induced *col1a1* expression (Fig. 6, *A* and *B*). Moreover, jasplakinolide, which stabilizes F-actin, dramatically increased basal αSMA levels (Fig. 6*A*), but TGFβ treatment did not result in a further increase in αSMA. By contrast, jasplakinolide did not affect basal *col1a1* expression and even inhibited the TGFβ1-induced increase of *col1a1* (Fig. 6*B*).

Actin polymerization downstream of Rac1 and Cdc42 is prominently promoted by the Arp2/3 complex and downstream of RhoA by formins of the mDia family. To probe the role of Arp2/3-mediated F-actin formation during myofibroblast differentiation, we deleted Arpc2, which is an essential component of the Arp2/3 complex (13, 14). Although Arpc2 was efficiently deleted (Fig. 6*C*), we did not observe an alteration in TGFβ-induced expression of αSMA or *col1a1* (Fig. 6, *D* and *E*).

CRISPR/Cas9-mediated cofilin targeting strongly increased stress fiber formation and αSMA levels but did not affect inducibility of αSMA by TGFβ1 (Fig. 6, *F* and *G*), confirming the notion that cofilin is not required for the TGFβ-induced increase of αSMA (Figs. 5*C* and 6*G*). CRISPR/Cas9-mediated deletion of the cofilin gene however did not affect *col1a1* expression (Fig. 6*H*). Downstream of RhoA, Rac1, and Cdc42, LIMK inhibits cofilin by phosphorylation. Loss of LIMK should therefore decrease cofilin phosphorylation, increase cofilin activity, decrease F-actin, and decrease αSMA, at least if one assumes that cofilin expression is unaltered. LIMK KO were made, and frameshifts in the coding region of the respective genes (*LIMK1* and *LIMK2*) were confirmed by sequencing of the genomic PCR fragments (Fig. S3*A*). Paradoxically, loss of LIMK1 increased basal and TGFβ-induced expression of αSMA, whereas LIMK2 KO had no influence (Fig. 6, *I* and *J*). Interestingly, only LIMK2 KO reduced pCofilin levels, indicat-

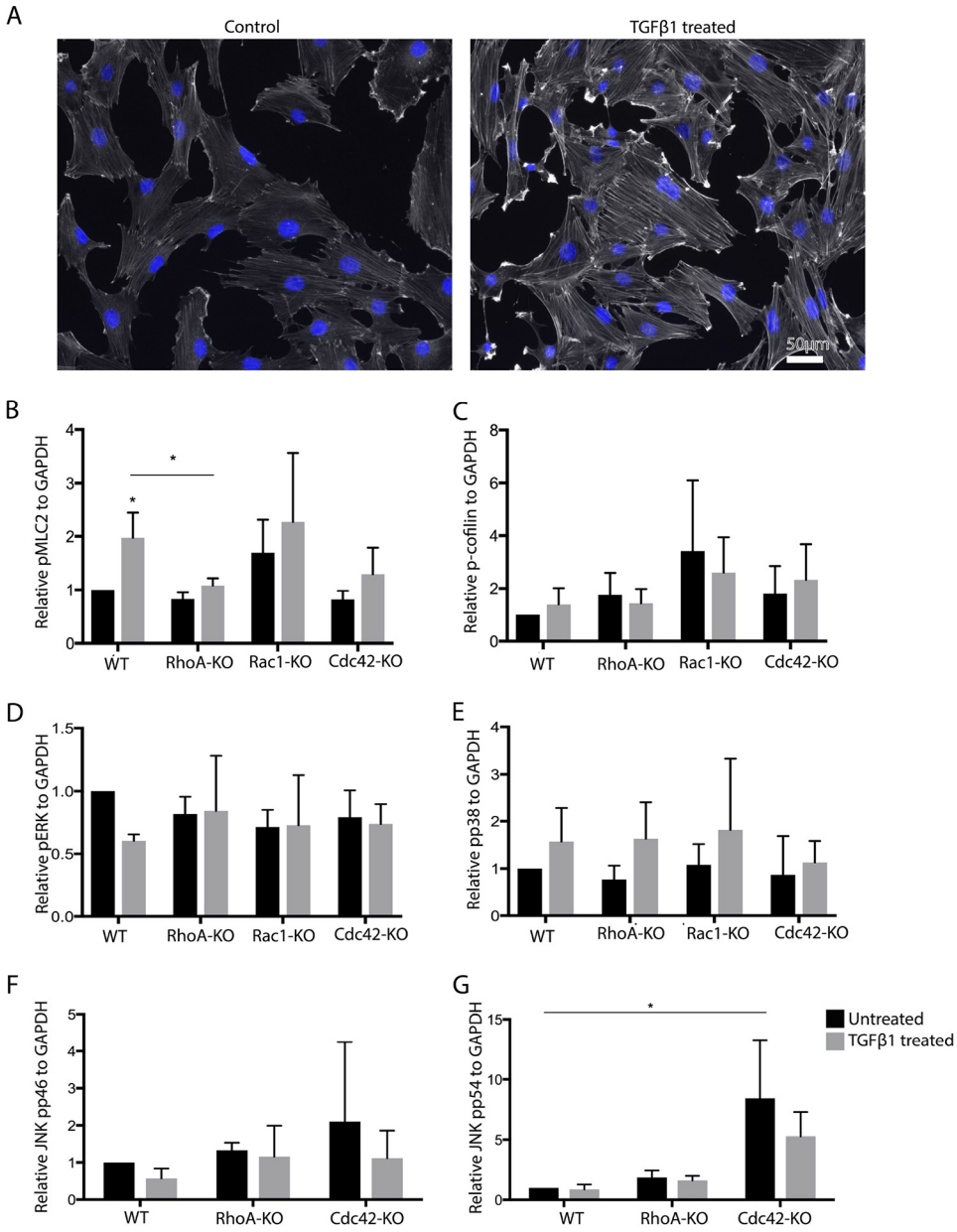

Figure 5. Cdc42-KO MSC display increased pJNK. *A*, F-actin of TGFβ1-treated and untreated MSC detected by fluorescently labeled phalloidin. *B–G*, quantifications of Western blot analyses of lysates of indicated MSC for pMLC2 (*B*), pCofilin (*C*), pERK (*D*), pp38 (*E*) JNK pp46 (*F*), and JNK pp54 (*G*). (*black bars*, 24-h TGFβ; *gray bars*, untreated; $n = 3/3$).

ing that LIMK2, but not LIMK1, is crucial for cofilin phosphorylation in MSC (Fig. 6*L*). LIMK1 KO, on the other hand, resulted in an increase of pCofilin, implying increased activation of LIMK2. Indeed, double knockout of LIMK1 and LIMK2 restored αSMA levels to that of WT cells (Fig. 6*K*). Conceivably, the deletion of LIMK1 was overcompensated by LIMK2, which was rescued by the additional deletion of LIMK2. Correspondingly, LIMK1 KO increased and LIMK2 or LIMK1/2 KO decreased F-actin in MSC (Fig. S3, *B* and *C*).

LIMK deletion did not influence TGFβ-induced *col1a1* expression (Fig. 6*M*). Finally, deletion of the MRTFa gene, confirmed by genomic sequencing of the targeted genomic region (Fig. S3), blocked TGFβ induction of αSMA but had no influence on *col1a1* mRNA (Fig. 6, *N* and *O*). Deletion of MRTFa did not interfere with the differentiation of MSC to adipocytes or osteoblasts (Fig. S6).

These data demonstrate that Arp2/3 complex-independent but F-actin/MRTFa-dependent signaling is crucial for TGFβ-induced αSMA expression in MSC. However, F-actin/MRTFa signaling is again dispensable for the stimulation of *col1a1* expression by TGFβ. Moreover, Rho-GTPase–dependent regulation of ADF/cofilin activity is not essential for the TGFβ-induced expression of αSMA.

TGFβ-induced cell contraction is required for increased actin polymerization

To understand the relationship between TGFβ-induced cell contraction, F-actin distribution, and αSMA expression, we

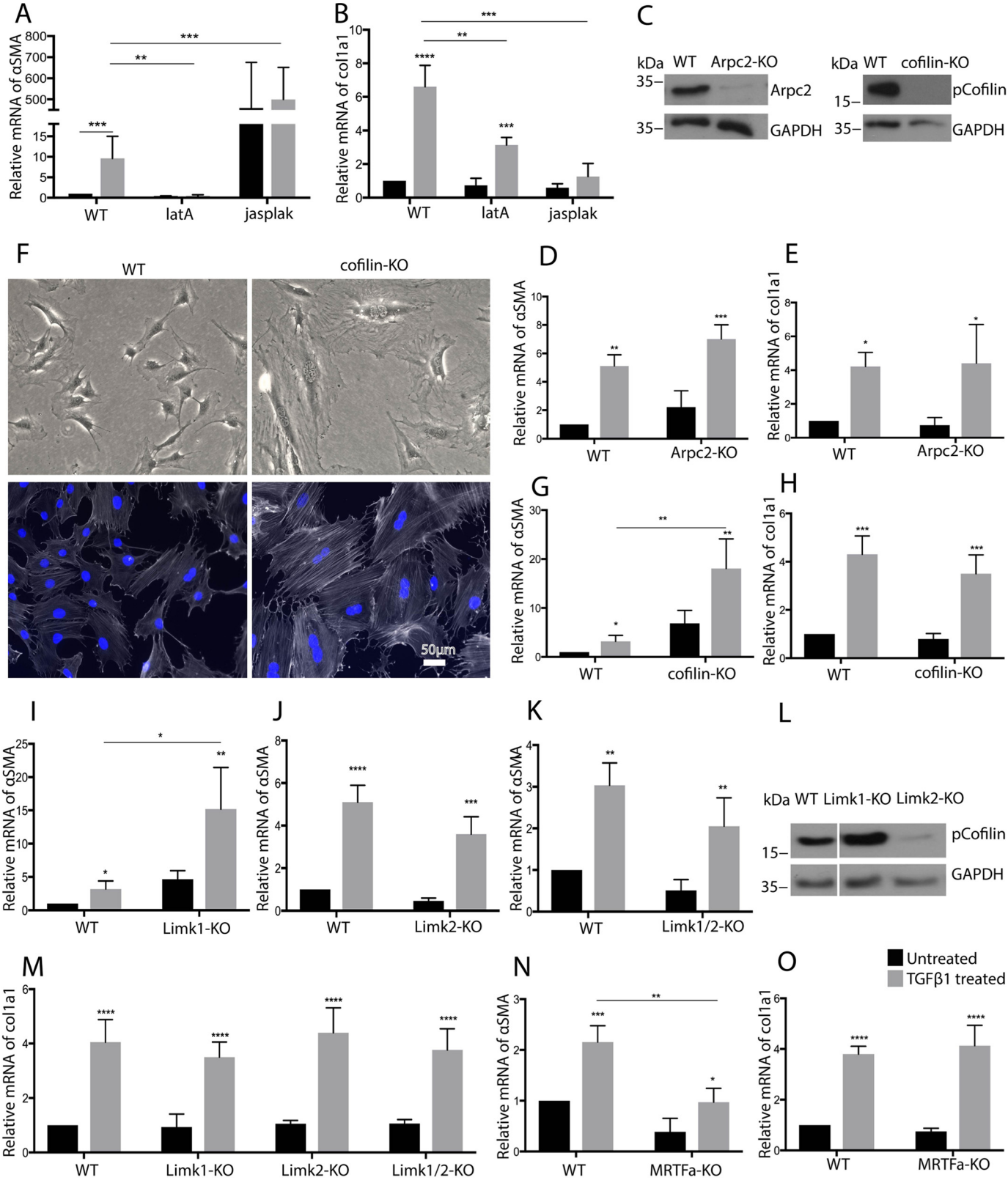

Figure 6. Cofilin is not required for TGFβ-induced expression of αSMA in MSC. *A*, *B*, *D*, *E*, *G–K*, and *M–O*, qRT-PCR analysis for indicated genes of WT cells treated with latrunculin A (*latA*) or jasplakinolide (*jasplak*) (*A* and *B*), Arpc2-KO (*D* and *E*), cofilin-KO (*G* and *H*), Limk1-KO (*I* and *M*), Limk2-KO (*J* and *M*), Limk1/2 KO (*K* and *M*), and MRTFa KO (*N* and *O*) ($n = 4/4$). *C*, representative Western blotting for the indicated proteins of MSC with knockout of Arpc2 or cofilin. *F*, *upper*, bright field microscopy of indicated MSC. *Lower*, F-actin (*white*) of indicated MSC, detected by fluorescently labeled phalloidin. Nuclear counterstaining (*blue*) by DAPI is shown. *L*, Western blotting for pCofilin of MSC with indicated KO. (*A–O*, *black bars*, 24-h TGFβ; *gray bars*, untreated). ****, $p < 0.0001$.

inhibited cell contraction directly by blebbistatin and indirectly by the ROCK inhibitor Y27632 or KO of contraction-promoting Rho GTPase effectors. Blebbistatin strongly reduced F-actin levels and prevented TGFβ-induced αSMA expression but did not affect *col1a1* expression (Fig. 7, *A*, *B*, and *E*). Similarly, inhibition of the RhoA effectors ROCK1 and ROCK2 by Y27632 inhibited stress fiber formation and effectively reduced TGFβ-induced αSMA expression but not *col1a1* expression (Fig. 7, *C*, *D*, and *E*). Individual knockout of ROCK1 and ROCK2 showed a partial reduction of pMLC2, F-actin, and αSMA, whereas the combined deletion of ROCK1 and ROCK2 had a stronger effect, indicating redundancy between ROCK1 and ROCK2 (Fig. 7, *F*, *G*, and *I–K*, and Fig. S4*A*). The combined deletion of ROCK1 and ROCK2 did not interfere with the differentiation of MSC to adipocytes or osteoblasts (Fig. S6).

Aside from ROCK, the Cdc42 effectors MRCKα and MRCKβ are also reported to regulate cell contraction in a fashion similar to ROCK. However, deletion of these genes showed little influence on pMLC2, F-actin, or αSMA (Fig. 7, *F*, *H*, and *L–N*, and Fig. S5*A*), indicating that Cdc42 affects cell contraction in MSC in a nonclassical manner. Importantly, none of the manipulations described above led to a significant change in basal or TGFβ-induced *col1a1* mRNA, corroborating that the regulation of αSMA and *col1a1* expression in MSC is distinct (Figs. S4*B* and S5*B*).

Discussion

This study on the TGFβ-induced differentiation of MSC to myofibroblasts revealed several surprising findings (Fig. S10). First, it shows that TGFβ-induced expression of αSMA and collagen 1 are differentially regulated in MSC, in contrast to fibroblasts. Secondly, it indicates that Rac1 and Cdc42 control TGFβ-induced αSMA expression in an opposite manner and independent of Arp2/3 complex–mediated actin polymerization. Thirdly, it demonstrates that the regulation of cofilin activity is not important for TGFβ-induced αSMA expression, contrary to earlier expectations. Fourthly, the data suggest that RhoA, Rac1, and Cdc42 control αSMA expression by a contraction-dependent pathway. Finally, this study reveals that Cdc42 and RhoA affect cytoplasmic retention and secretion of collagen I in MSC.

Although MRTFa is required for collagen I expression in lung fibroblasts and in myofibroblasts derived from scleroderma (10, 11), collagen I expression in our MSC line was clearly independent of MRTFa, although TGFβ-induced αSMA expression was highly dependent on MRTFa. On the other hand, canonical Smad4-dependent TGFβ signaling was essential for both collagen I as well as αSMA expression. This fits with an earlier report on mesangial cells showing that Smad4 is required for TGFβ-induced collagen I expression (15). It is well-known that the regulation of TGFβ-dependent genes is strongly context-dependent and cell type–specific (8). Synergistic interaction of MRTFa with Smad4 signaling at the collagen I promoter is required in fibroblasts and myofibroblasts (10, 11) but, as our data reveal, not in MSC. WT MSC will therefore be resistant to fibrosis-inhibiting drugs targeting the RhoA/ROCK/MRTFa pathway. It will be interesting to investigate why MSC do not require MRTFa activation for *col1a1* expression. It is possible that MRTFa removes an inhibitory transcription factor or epigenetic mark from the *col1a1* gene locus in fibroblasts but not in MSC. Such a mechanism was found in genes for master regulators of embryonic stem cell differentiation, where the Smad3-binding factor TRIM33 disables repressive histone marks (16).

Introduction of this *col1a1* gene inhibitory signal to MSC will make their collagen I expression dependent on the activation of RhoA/ROCK/MRTFa. This could increase the efficiency of ROCK inhibitors as antifibrotic drugs. ROCK inhibitors such as fasudil show some efficacy in mouse and rat models of fibrosis (17), but no reports on clinical efficacy in humans have been published up to now.

Polymerization and depolymerization of F-actin and thus MRTFa activation is not only regulated by RhoA but also by Rac1 and Cdc42 (18). It was therefore expected that deletion of Rac1 or Cdc42 might decrease MRTFa-dependent αSMA expression by reducing Arp2/3-dependent actin polymerization or by increasing actin depolymerization via reduced phosphorylation of cofilin. Unexpectedly, our data revealed that Rac1 and Cdc42 modulate F-actin amounts and αSMA expression but in an Arp2/3- and cofilin-independent manner. Moreover, Cdc42 and Rac1 had an opposite effect on actin polymerization, suggesting that they regulate F-actin in MSC in a rather unconventional manner, probably dependent on cell contraction. MRCKα and MRCKβ are ROCK-like effectors of Cdc42 that mediate contraction (19). In MSC, however, MRCKα and MRCKβ are apparently not involved in the regulation of myofibroblast differentiation. Although the molecular details of the regulation of contraction by Cdc42 and Rac1 in MSC remain to be elucidated, our data clearly identify Cdc42 as a potential novel drug target for fibrosis therapy.

We observed increased JNK phosphorylation in Cdc42 KO MSC after 24 h of TGFβ stimulation. However, control cells or cells lacking RhoA or Rac1 showed no effect, although a transient, earlier increase cannot be excluded. JNK activation leads, among other pathways, to phosphorylation and activation of c-Jun, reported to inhibit canonical TGFβ signaling (20, 21). Indeed, Cdc42-null MSC showed a certain reduction of collagen I expression, which may be related to the increased JNK activation. On the other hand, the JNK inhibitor CC-401 significantly inhibited renal fibrosis in a kidney fibrosis model (22), suggesting a profibrotic function of JNK. Moreover, JNK activation is a well-known part of noncanonical TGFβ signaling and has been described as crucial for TGFβ-induced myofibroblast development *in vitro* (23). The molecular mechanism of Cdc42 loss-of-function– dependent JNK activation is not clear, as the latter is thus far considered a downstream effector of Cdc42 (24). JNK inhibitors employed in Cdc42-null MSC may reveal the relevance of JNK for myofibroblast differentiation.

Cofilin inhibition by phosphorylation commonly promotes F-actin formation (25), expected to result in increased MRTFa activation and increased MRTFa-dependent gene expression. Indeed, deletion of cofilin (cofilin-1) in MSC increased F-actin and αSMA expression, suggesting that MRTFa is able to stimulate αSMA expression also in the absence of exogenous TGFβ. However, the addition of TGFβ resulted in a similar -fold change in αSMA expression as in WT cells, indicating that the

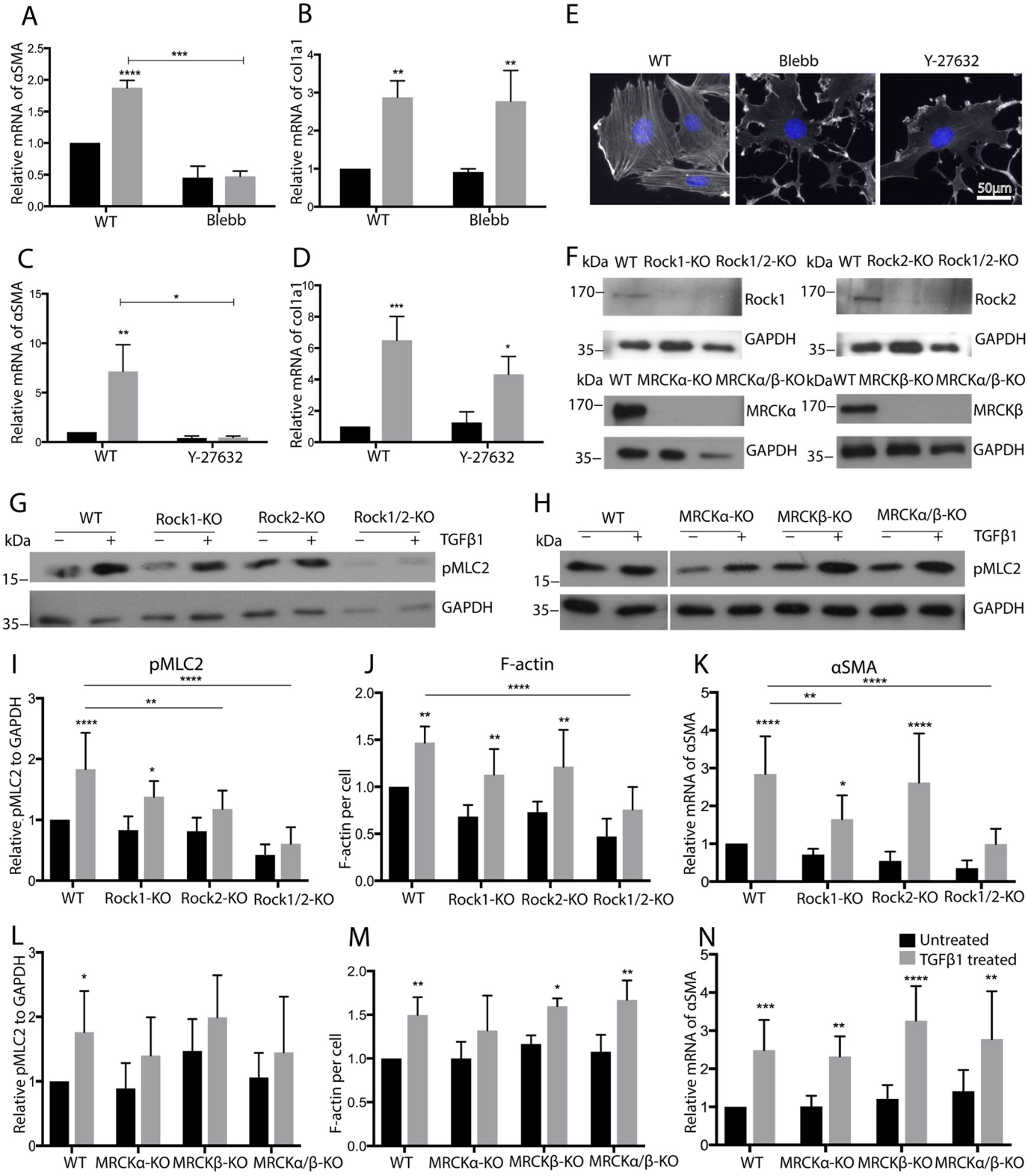

Figure 7. TGFβ-induced αSMA induction of MSC correlates with changes in contraction and F-actin. *A–D*, qRT-PCR analysis for the indicated genes of WT cells treated with blebbistatin (*Blebb* (*A* and *B*)) or Y-27632 (*C* and *D*) ($n = 3/3$). *E*, F-actin of MSC treated with blebbistatin or Y-27632, detected by fluorescently labeled phalloidin. *F*, representative Western blotting for the indicated proteins of MSC with knockout of Rock1, Rock2, MRCKα, and MRCKβ. *G–I* and *L*, representative Western blotting and quantification of lysates of indicated cells for pMLC2 ($n = 6/6$). *J* and *M*, quantification of phalloidin staining of indicated MSC ($n = 5/5$). *K* and *N*, qRT-PCR analysis for αSMA of MSC with indicated KO ($n = 5/5$). *A–D*, *J*, *K*, *M*, and *N*, *black bars*, 24-h TGFβ; *I* and *L*, *black bars*, 2-h TGFβ; *gray bars*, untreated. ****, $p < 0.0001$.

TGFβ induction of αSMA expression is largely independent of cofilin. Normal αSMA expression after deletion of both LIMK genes, negative regulators of cofilin downstream of RhoA, Rac1, and Cdc42, supported this notion. Interestingly, the deletion of RhoA, Rac1, or Cdc42 did not lead to changes in the basal levels of TGFβ-induced phosphocofilin, neither in the presence or absence of TGFβ (at 2 h), although all three Rho GTPases affected the F-actin levels. These data suggest that the importance of Rho GTPase–dependent cofilin regulation is highly cell type–dependent.

A possible model explaining our data is that RhoA, Rac1, and Cdc42 regulate αSMA expression in MSC via a RhoA/ROCK/pMLC2/F-actin/MRTFa pathway. Apparently, increased contraction of F-actin prevents its depolymerization, as already suggested previously (26). Because Arp2/3 complex–dependent actin polymerization is not required for TGFβ-induced αSMA expression, formin-mediated stress fiber formation could be important for regulating MRTFa in MSC, which would fit the correlation between stress fiber formation and αSMA expression observed here and the well-known correlation between contraction and stress fiber formation (27). Because Cdc42- and Rac1-dependent actin assembly operating in TGFβ-induced differentiation of MSC is not controlled through conventional regulation by Arp2/3, cofilin, or MRCK-dependent regulation of contraction, it is possible that they act upstream of RhoA. Cross-talk between Rho GTPases is well-established in various conditions and cell types and may involve competition for GDIs, GDFs, and GAPs (28, 29).

Finally, we observed an accumulation of intracellular collagen I in Cdc42 KO and RhoA KO cells. In Cdc42-null MSC, this correlated with a decreased amount of collagen I in the cell supernatant, but this was not obvious in RhoA-null cells. It was reported previously that in smooth muscle cells Cdc42 regulates collagen I secretion via PKCδ (30). It appears that a similar mechanism might take place in MSC. Cdc42 is known to regulate transport between the endoplasmic reticulum and Golgi (31), whereas RhoA has not been reported to be involved in constitutive secretion. In any case, the secretion defect in Cdc42-null MSC further increases the interest in Cdc42 as a potential drug target for fibrosis therapy.

In conclusion, not only RhoA but also Rac1 and Cdc42 are important for noncanonical TGFβ signaling, at least in MSC differentiation into myofibroblasts. Noncanonical TGFβ signaling differentially regulates expression of αSMA and *col1a1* in MSC, in contrast to fibroblasts and myofibroblasts, which may be relevant for fibrosis therapies. Finally, Cdc42 emerges as an interesting drug target for fibrotic diseases, as it may interfere with myofibroblast differentiation as well as collagen I secretion.

Experimental procedures

MSC isolation and culture

Primary mouse MSC were isolated from bone as described (32). Primary and immortalized MSC were cultured in MSC growth medium (αMEM (Gibco 32561-029), 10% fetal bovine serum (Thermo Fisher Scientific 12662011), and 100 units/ml penicillin-streptomycin (Gibco 15140)) at 37 °C and 5% CO_2. Primary MSCs were split 1:3 (primary) or 1:4 (MSC line) after reaching 90% confluence. For detachment, MSC were washed once in a 10-cm tissue culture dish (Greiner Cellstar P7612) with 2 ml of warm PBS and then incubated with 1 ml of 5% trypsin-EDTA (Gibco 25200-056) for exactly 2 min at 37 °C. Trypsin digestion was stopped by adding 1 ml of MSC growth medium. Because contaminating macrophages mostly will not detach during this time, MSCs would be enriched by passaging.

MSC differentiation

The differentiation potential of MSC to adipocytes or osteoblasts was measured using corresponding kits from STEMCELL Technologies (STEMCELL catalog no. 05503 and 05504). Myofibroblast differentiation of MSC was stimulated by 5 ng/ml human TGFβ1 (Chinese hamster ovary cell line–derived, Ala^{279}–Ser^{390}; R&D Systems 240-B-002) for 24 or 72 h.

CRISPR/Cas9-mediated genome editing in MSC

Gene deletion in MSC was mediated by lentiviruses transducing CRISPR/Cas9 gene-editing constructs (33). Guide RNA (gRNA) targeting the coding region close to the translation start site of the respective gene of interest were designed using the CRISPRSCAN program (34) as follows: nontarget control, CACCGGTATTACTGATATTGGTGGG; RhoA, CACCGGATAAGAGAGAGGCCGCAGG; Rac1, CACCGACGGTGGGGATGTACTCTCC; Cdc42, CACCGAAAGCTGGCGCGGGATCTGA; Rock1, CACCGGCCGATTTGGGATCCCGCAGC; Rock2, CACCGGGGGTTCTGAAATCACAAGG; MRCKa, CACCGGGTCCGGAGAAGTGCGTTTG; MRCKb, CACCGGGGGCGGAGTTCCTCGAGTG; Smad2, CACCGGATGGAAAAAATCAGCCGGT; Smad3, CACCGGGTCGGGCCATCGCCACAGG; Smad4, CACCGGATGTGTCATAGACAAGGTG; MRTFa, CACCGGGAGGAGGCTATCATTGGTG; PAK1, CACCGGGGCGTGGAGCAATCACTGG; Limk1, CACCGGGGTGGGAGCCGGGTGAGTC; Limk2, CACCGGGTGAGCATGAGCGTGTGTC; cofilin, CACCGGGTCCCTCAGGCCTCTGGTG; and Aprc2, CACCGGGTGACGACGATGTGGTCAT. Annealed DNA oligonucleotides containing the gRNA sequence were then cloned into the lentiCRISPR v2 vector (addgene 62988) as described earlier (33). When needed, the puromycin resistance was exchanged against a blasticidin resistance gene.

Lentivirus was produced by transfection of subconfluent HEK293 cells with 0.8 μg of lentiCRISPRv2, as described above, or 0.8 μg of pLenti.PGK.LifeAct-GFP (addgene 51010), 0.6 PAX2 (addgene 12260), and 0.6 μg of VSVG plasmid (addgene 8454) in the presence of 8 μg of polyethylenimine (Polyplus) in 200 μl of optiMEM (Thermo Fisher Scientific 11058021). Virus-containing supernatant was collected after 24 and 48 h, filtered through a 0.45-μm cellulose acetate membrane filter (VWR 28145-481) to remove cells, and used directly for the transduction of MSC. Supernatant of 40–60% confluent MSC seeded the previous day was aspirated, and 1–2 ml of filtrated virus supernatant and 4 μl of 4 μg/ml hexadimethrine bromide (Polybrene; Sigma 107689) in PBS were added to each well of a 6-well plate. After 1 day, the supernatant was replaced with MSC growth medium. 48 h after transduction, antibiotic selection was started with 4 μg/ml puromycin for 2 days or 8 μg/ml

blasticidin for 5 days. MSC expressing fluorescent LifeAct were not selected by antibiotics but were identified by fluorescence.

Fast-cycling Rho GTPase mutants

cDNAs encoding HA-tagged fast-cycling Rho GTPase mutants (RhoA (F30L), Rac1 (F28L), and Cdc42 (F28L) (35)) were cloned together with IRES-EGFP into the lentiviral expression vector pRRLsin, kindly obtained from Dr. Didier Trono (EPFL, Lausanne, Switzerland). Lentiviral transduction of MSC was carried out as described above. Efficient transduction was confirmed by assessing EGFP expression using fluorescence microscopy.

F-actin staining

Sterile coverslips were placed into the wells of a 24-well plate with 500 μl of 50 μg/ml poly-L-lysine solution. After 1 h of incubation at 37 °C, the coating solution was removed, and the surface was allowed to dry. 5000 MSC were plated on each of the glass slides in 1 ml of MSC growth medium. The next day, the MSC were stimulated with 5 ng/ml TGFβ1 (R&D Systems 240-B-002) for 24 h, and then MSC were fixed with 4% paraformaldehyde in PBS for 10 min at room temperature and stored at 4 °C. To stain for F-actin, MSC on coverslips were incubated with 1:200 diluted phalloidin–Atto 568 (Thermo Fisher Scientific A12380) in PBS with 2% BSA and 0.5% Triton for 1 h at room temperature. Coverslips were washed with 1 ml of PBS for 10 s and then mounted on a glass slide using mounting buffer (Sigma F6057). For each sample, five randomly chosen non-overlapping images were taken. For a given experiment, all images were taken with the same exposure time using a fluorescent channel appropriate for detection of Alexa Fluor 568 by conventional fluorescence microscopy (Axio Imager 2, Zeiss). Total F-actin signal was measured on each slide using ImageJ; each cell was selected manually, and the integrated density in each cell on the red channel was measured and quantified.

Flow cytometry

MSC were detached by trypsinization and then resuspended in PBS containing 1% BSA at 1 million cells/ml. To block the binding of antibodies to cellular Fc receptors, MSC were preincubated with 1 μg of anti-mouse CD16/CD32 (eBioscience 14-0161-85) per 100 μl of MSC for 15 min at 4 °C in 1.5 ml of Eppendorf tubes. Then, fluorescently labeled antibodies at the indicated dilutions were added. The following rat anti-mouse antibodies (all from eBioscience) were used: CD105 (catalog no. 12-1051-81), CD11b (17-0112-81), CD44 (17-0441-81), CD45 (12-0454-82), Sca1 (17-5981-83), IgG2a isotype control allophycocyanin, and IgG2a isotype control phycoerythrin (12-4321-81). After mixing, the solution was protected from light and incubated for at least 30 min at 4 °C. Cells were washed by adding 3 volumes of PBS, 1%BSA, pelleted by centrifugation at 340 × *g* for 5 min, resuspended and fixed with 1% paraformaldehyde in PBS for 10 min at room temperature, pelleted by centrifugation, and resuspended in 500 μl of PBS. Cellular fluorescence was measured using CellQuest software on a BD FACSCalibur. Data analysis was carried out with the FlowJo 10.2 program (FlowJo, LLC).

Western blotting

Cell lysate samples, around 10–20 μg/lane, were separated by 12% SDS-PAGE and transferred at 4 °C to polyvinylidene fluoride membranes. The membranes were blocked using 5% milk in TBS, 0.05% Tween (TBS-T) for 60 min and incubated overnight at 4 °C with the indicated primary antibodies. RhoA (sc-418), GAPDH (sc-25778), Rock1 (sc-5560), Rock2 (sc-5561), MRCKa (sc-374568), MRCKb (sc-374597), and pp38 (sc-17852-R) were from Santa Cruz Biotechnology. Rac1 (catalog no. 610650) and Cdc42 (no. 610929) were from BD Biosciences; pMLC2 (no. 3674), pCofilin (no. 3311), pSmad2 (no. 3108S), pJNK (no. 9251S), pERK (no. 9101S), and PAK1 (no. 2602) from Cell Signaling; αSMA (GTX100034) from GeneTex; collagen I (ab34710), Smad3 (ab28379), Smad4 (ab40759), and Arpc2 (ab133315) from Abcam; and pPAK1 (PA5-12844) and pPAK4 (PA5-36865) from Thermo Fisher Scientific. Following three 15-min washing steps with TBS-T, the membranes were incubated with the corresponding secondary antibodies (Jackson Immunoresearch) for 60 min. Following at least three 15-min washing steps, the membranes were treated with Luminata™ Western horseradish peroxidase chemiluminescence substrate detection reagent (Millipore) for 1 min at room temperature. Luminescence was detected with medical X-ray film (Agfa).

Movies

15,000 WT, KO, and LifeAct-expressing MSC were plated in each well of 4-well glass-bottom dishes (Thermo Fisher Scientific 154461PK) coated with 10 μg/ml human fibronectin (Roche Life Science) 1 day before live cell imaging. Time-lapse microscopy was performed on an Axio Observer (Zeiss) equipped with an automated stage, a VIS-LED light source for phase-contrast optics, and light source for GFP, and a Coolsnap-HQ2 camera (Photometrics) driven by VisiView software (Visitron Systems). The microscope was equipped additionally with a 37 °C incubator and CO_2-aerated lid and switched on at least 1 h before the start of the experiment for equilibration and to avoid focus drifts during the experiment. Two channels of phase-contrast and GFP fluorescence movies were acquired using a ×10/0, 3NA objective on several randomly chosen positions per condition, at a frame rate of 6/h (100 images in total per region). Image stacks were then transformed into AVI movie files using ImageJ software.

Statistics

Data were presented as mean ± S.E. Unpaired, two-tailed Student's *t* tests were used for comparisons between two groups. For multiple comparisons, two-way analysis of variance with Tukey's multiple comparisons was applied. Statistical analysis was done using GraphPad Prism. The following indications of significance were used throughout this study (Figs. 2–7): *, $p < 0.05$; **, $p < 0.01$; ***, $p < 0.001$.

Author contributions—J. G. and C. B. conceptualization; J. G. and K. R. data curation; J. G. formal analysis; J. G. and K. R. validation; J. G. investigation; J. G., L. B., M. A., M. Q. K., M. S., and K. R. methodology; J. G., K. R., and C. B. writing-review and editing; L. B., K. R., and C. B. supervision; K. R. and C. B. resources; C. B. funding acquisition; C. B. writing-original draft; C. B. project administration.

Acknowledgments—We thank Volkan Turan for expert technical help and Dr. Didier Trono (EPFL, Switzerland) for providing a lentiviral expression vector.

References

1. Nanthakumar, C. B., Hatley, R. J., Lemma, S., Gauldie, J., Marshall, R. P., and Macdonald, S. J. (2015) Dissecting fibrosis: Therapeutic insights from the small-molecule toolbox. *Nat. Rev. Drug Discov.* **14,** 693–720 CrossRef Medline
2. Rosenbloom, J., Macarak, E., Piera-Velazquez, S., and Jimenez, S. A. (2017) Human fibrotic diseases: Current challenges in fibrosis research. *Methods Mol. Biol.* **1627,** 1–23 CrossRef Medline
3. Tsochatzis, E. A., Crossan, C., Longworth, L., Gurusamy, K., Rodriguez-Peralvarez, M., Mantzoukis, K., O'Brien, J., Thalassinos, E., Papastergiou, V., Noel-Storr, A., Davidson, B., and Burroughs, A. K. (2014) Cost-effectiveness of noninvasive liver fibrosis tests for treatment decisions in patients with chronic hepatitis C. *Hepatology* **60,** 832–843 CrossRef Medline
4. Hinz, B. (2016) Myofibroblasts. *Exp. Eye Res.* **142,** 56–70 CrossRef Medline
5. Kramann, R., Schneider, R. K., DiRocco, D. P., Machado, F., Fleig, S., Bondzie, P. A., Henderson, J. M., Ebert, B. L., and Humphreys, B. D. (2015) Perivascular Gli1+ progenitors are key contributors to injury-induced organ fibrosis. *Cell Stem Cell* **16,** 51–66 CrossRef Medline
6. Desai, V. D., Hsia, H. C., and Schwarzbauer, J. E. (2014) Reversible modulation of myofibroblast differentiation in adipose-derived mesenchymal stem cells. *PLoS ONE* **9,** e86865 CrossRef Medline
7. Kim, W., Barron, D. A., San Martin, R., Chan, K. S., Tran, L. L., Yang, F., Ressler, S. J., and Rowley, D. R. (2014) RUNX1 is essential for mesenchymal stem cell proliferation and myofibroblast differentiation. *Proc. Natl. Acad. Sci. U.S.A.* **111,** 16389–16394 CrossRef Medline
8. Massagué, J. (2012) TGFβ signalling in context. *Nat. Rev. Mol. Cell Biol.* **13,** 616–630 CrossRef Medline
9. Esnault, C., Stewart, A., Gualdrini, F., East, P., Horswell, S., Matthews, N., and Treisman, R. (2014) Rho-actin signaling to the MRTF coactivators dominates the immediate transcriptional response to serum in fibroblasts. *Genes Dev.* **28,** 943–958 CrossRef Medline
10. Luchsinger, L. L., Patenaude, C. A., Smith, B. D., and Layne, M. D. (2011) Myocardin-related transcription factor-A complexes activate type I collagen expression in lung fibroblasts. *J. Biol. Chem.* **286,** 44116–44125 CrossRef Medline
11. Shiwen, X., Stratton, R., Nikitorowicz-Buniak, J., Ahmed-Abdi, B., Ponticos, M., Denton, C., Abraham, D., Takahashi, A., Suki, B., Layne, M. D., Lafyatis, R., and Smith, B. D. (2015) A role of myocardin-related transcription factor-A (MRTF-A) in scleroderma-related fibrosis. *PLoS ONE* **10,** e0126015 CrossRef Medline
12. Ni, J., Dong, Z., Han, W., Kondrikov, D., and Su, Y. (2013) The role of RhoA and cytoskeleton in myofibroblast transformation in hyperoxic lung fibrosis. *Free Radic. Biol. Med.* **61,** 26–39 CrossRef Medline
13. Gournier, H., Goley, E. D., Niederstrasser, H., Trinh, T., and Welch, M. D. (2001) Reconstitution of human Arp2/3 complex reveals critical roles of individual subunits in complex structure and activity. *Mol. Cell* **8,** 1041–1052 CrossRef Medline
14. Rotty, J. D., Wu, C., Haynes, E. M., Suarez, C., Winkelman, J. D., Johnson, H. E., Haugh, J. M., Kovar, D. R., and Bear, J. E. (2015) Profilin-1 serves as a gatekeeper for actin assembly by Arp2/3-dependent and -independent pathways. *Dev. Cell* **32,** 54–67 CrossRef Medline
15. Tsuchida, K., Zhu, Y., Siva, S., Dunn, S. R., and Sharma, K. (2003) Role of Smad4 on TGF-β-induced extracellular matrix stimulation in mesangial cells. *Kidney Int.* **63,** 2000–2009 CrossRef Medline
16. Xi, Q., Wang, Z., Zaromytidou, A. I., Zhang, X. H., Chow-Tsang, L. F., Liu, J. X., Kim, H., Barlas, A., Manova-Todorova, K., Kaartinen, V., Studer, L., Mark, W., Patel, D. J., and Massagué, J. (2011) A poised chromatin platform for TGF-β access to master regulators. *Cell* **147,** 1511–1524 CrossRef Medline
17. Knipe, R. S., Tager, A. M., and Liao, J. K. (2015) The Rho kinases: critical mediators of multiple profibrotic processes and rational targets for new therapies for pulmonary fibrosis. *Pharmacol. Rev.* **67,** 103–117 Medline
18. Ridley, A. J. (2006) Rho GTPases and actin dynamics in membrane protrusions and vesicle trafficking. *Trends Cell Biol.* **16,** 522–529 CrossRef Medline
19. Unbekandt, M., and Olson, M. F. (2014) The actin-myosin regulatory MRCK kinases: Regulation, biological functions and associations with human cancer. *J. Mol. Med. (Berl.)* **92,** 217–225 Medline
20. Leask, A., Holmes, A., Black, C. M., and Abraham, D. J. (2003) Connective tissue growth factor gene regulation. Requirements for its induction by transforming growth factor-β 2 in fibroblasts. *J. Biol. Chem.* **278,** 13008–13015 CrossRef Medline
21. Verrecchia, F., Tacheau, C., Schorpp-Kistner, M., Angel, P., and Mauviel, A. (2001) Induction of the AP-1 members c-Jun and JunB by TGF-β/Smad suppresses early Smad-driven gene activation. *Oncogene* **20,** 2205–2211 CrossRef Medline
22. Ma, F. Y., Flanc, R. S., Tesch, G. H., Han, Y., Atkins, R. C., Bennett, B. L., Friedman, G. C., Fan, J. H., and Nikolic-Paterson, D. J. (2007) A pathogenic role for c-Jun amino-terminal kinase signaling in renal fibrosis and tubular cell apoptosis. *J. Am. Soc. Nephrol.* **18,** 472–484 CrossRef Medline
23. Hashimoto, S., Gon, Y., Takeshita, I., Matsumoto, K., Maruoka, S., and Horie, T. (2001) Transforming growth Factor-beta1 induces phenotypic modulation of human lung fibroblasts to myofibroblast through a c-Jun-NH2-terminal kinase-dependent pathway. *Am. J. Respir. Crit. Care Med.* **163,** 152–157 CrossRef Medline
24. Coso, O. A., Chiariello, M., Yu, J. C., Teramoto, H., Crespo, P., Xu, N., Miki, T., and Gutkind, J. S. (1995) The small GTP-binding proteins Rac1 and Cdc42 regulate the activity of the JNK/SAPK signaling pathway. *Cell* **81,** 1137–1146 CrossRef Medline
25. Kanellos, G., and Frame, M. C. (2016) Cellular functions of the ADF/cofilin family at a glance. *J. Cell Sci.* **129,** 3211–3218 CrossRef Medline
26. Hayakawa, K., Tatsumi, H., and Sokabe, M. (2011) Actin filaments function as a tension sensor by tension-dependent binding of cofilin to the filament. *J. Cell Biol.* **195,** 721–727 CrossRefMedline
27. Bershadsky, A. D., Ballestrem, C., Carramusa, L., Zilberman, Y., Gilquin, B., Khochbin, S., Alexandrova, A. Y., Verkhovsky, A. B., Shemesh, T., and Kozlov, M. M. (2006) Assembly and mechanosensory function of focal adhesions: Experiments and models. *Eur. J. Cell Biol.* **85,** 165–173 CrossRef Medline
28. Garcia-Mata, R., Boulter, E., and Burridge, K. (2011) The 'invisible hand': Regulation of RHO GTPases by RHOGDIs. *Nat. Rev. Mol. Cell Biol.* **12,** 493–504 CrossRef Medline
29. Lawson, C. D., and Burridge, K. (2014) The on-off relationship of Rho and Rac during integrin-mediated adhesion and cell migration. *Small GTPases* **5,** e27958 CrossRef Medline
30. Lengfeld, J., Wang, Q., Zohlman, A., Salvarezza, S., Morgan, S., Ren, J., Kato, K., Rodriguez-Boulan, E., and Liu, B. (2012) Protein kinase C δ regulates the release of collagen type I from vascular smooth muscle cells via regulation of Cdc42. *Mol. Biol. Cell* **23,** 1955–1963 CrossRef Medline
31. Wu, W. J., Erickson, J. W., Lin, R., and Cerione, R. A. (2000) The γ-subunit of the coatomer complex binds Cdc42 to mediate transformation. *Nature* **405,** 800–804 CrossRef Medline
32. Zhu, H., Guo, Z. K., Jiang, X. X., Li, H., Wang, X. Y., Yao, H. Y., Zhang, Y., and Mao, N. (2010) A protocol for isolation and culture of mesenchymal stem cells from mouse compact bone. *Nat. Protoc.* **5,** 550–560 CrossRef Medline
33. Ran, F. A., Hsu, P. D., Wright, J., Agarwala, V., Scott, D. A., and Zhang, F. (2013) Genome engineering using the CRISPR-Cas9 system. *Nat. Protoc.* **8,** 2281–2308 CrossRef Medline
34. Moreno-Mateos, M. A., Vejnar, C. E., Beaudoin, J. D., Fernandez, J. P., Mis, E. K., Khokha, M. K., and Giraldez, A. J. (2015) CRISPRscan: Designing highly efficient sgRNAs for CRISPR-Cas9 targeting *in vivo*. *Nat. Methods* **12,** 982–988 CrossRef Medline
35. Lin, R., Cerione, R. A., and Manor, D. (1999) Specific contributions of the small GTPases Rho, Rac, and Cdc42 to Dbl transformation. *J. Biol. Chem.* **274,** 23633–23641 CrossRef Medline
36. Zhang, Y. E. (2017) Non-Smad signaling pathways of the TGF-β family. *Cold Spring Harb. Perspect. Biol.* **9,** a022129 CrossRef Medline